Model Identification and Control for a Quarter Car Test Rig of Series Active Variable Geometry Suspension

Min Yu * Simos A. Evangelou * Daniele Dini **

** Department of Electrical and Electronic Engineering, Imperial College London, London SW7 2AZ, UK (e-mail: m.yu14@ imperial.ac.uk, s.evangelou@imperial.ac.uk).*
*** Department of Mechanical Engineering, Imperial College London, London SW7 2AZ, UK (e-mail: d.dini@imperial.ac.uk).*

Abstract: In this paper, a quarter car test rig is utilized to perform an experimental study of the single-link variant of the Series Active Variable Geometry Suspension (SAVGS). A nonlinear model of the test rig is identified with the use of a theoretical quarter car model and the rig's experimental frequency response. A linear equivalent modeling method that compensates the geometric nonlinearity is also adopted to synthesize an H-infinity control scheme. The controller actively adjusts the single-link velocity in the SAVGS to improve the suspension performance. Experiments are performed to evaluate the SAVGS practical feasibility, the performance improvement, the accuracy of the nonlinear model and the controller's robustness.

Keywords: Active vehicle suspension, quarter car test rig, nonlinear model identification, robust control application, experimental validation.

1. INTRODUCTION

Vehicle suspension is the system of spring-damper units and linkage arms that connects a car body to its wheel and allows relative motion between the two (Sharp et al., 1987). The suspension directly affects drive comfort (vertical car body acceleration) and handling ability (tire normal load variation).

In recent decades, active suspensions have been widely studied to improve vehicle dynamics (Elbeheiry et al., 1995): pure active suspensions utilize a separate actuator, which can exert an independent force onto the suspension linkages; semi-active suspensions actively adjust the damping coefficient, by using technologies such as magneto-rheological fluids. More recently, a new Series Active Variable Geometry Suspension (SAVGS) has been proposed (Evangelou et al., 2011). As shown in Fig. 1, a rotary single-link is introduced in series with the spring-damper unit, while the other end of this link ('G') is fixed on the chassis. The single-link is driven by a rotary electromechanical actuator to provide increments to the force provided by the passive suspension strut. The SAVGS has been proven to be a potential alternative solution for active suspensions (Arana et al., 2014, 2015), due to: 1) significant performance improvement, 2) small increment in the sprung mass and no increment in the unsprung mass, 3) low power demand, and 4) fail-safe operation.

In previous work (Arana, 2015), virtual prototyping and control of the SAVGS system have been performed by utilizing respectively mathematical models of the system and model-based robust control methodologies. In this paper, an experimental study of the SAVGS is performed, with the aim to evaluate its practical feasibility, the mathematical models' accuracy, and the controllers' robustness. The main contributions are: 1) the SAVGS single-link implementation in a test rig, 2) the nonlinear model identification of the quarter car test rig, 3) the robust control application to the SAVGS test rig, and 4) the initial experimental validation with both the passive and the active cases considered.

The remainder of this paper is organized as follows. Section 2 introduces the quarter car with SAVGS test rig. Section 3 identifies the nonlinear model of the quarter car test rig. Section 4 utilizes a linear equivalent model and synthesizes an H-infinity scheme for the SAVGS control. Section 5 discusses the experiment results. Conclusions and future work are provided in Section 6.

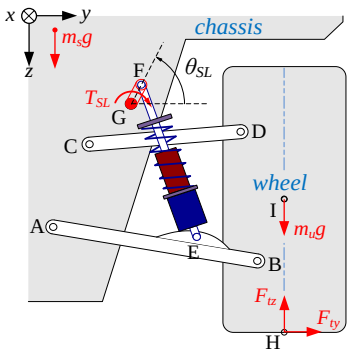

Fig. 1. The SAVGS application to a quarter car model with double wishbone suspension (Arana et al., 2015).

2. QUARTER CAR TEST RIG

In this section, the SAVGS quarter car test rig and the single-link variant implementation, for the experimental study, are described concisely.

2.1 Quarter Car Test Rig

Quarter car test rigs are commonly utilized for active suspensions studies (Fischer et al., 2004). However, two major issues exist in previous work. Firstly, the suspension kinematics is simplified into two pure vertical motions, thus the geometric nonlinearity and the installation ratio (Dixon, 2009) are not included. Secondly, the mass parameters are scaled down (e.g. the sprung mass) and therefore the load level of the active components cannot be accurately reflected.

With regards to the SAVGS, the spring-damper force as well as the installation ratio are changing with the rotation of the single-link, thus the suspension geometry must be considered. The SAVGS test rig is constructed based on a high performance sports car, with the specific parameter set used shown in Table I in the Appendix. As shown in Fig. 2, the primary mechanical parts in this rig are: 1) the supporting frame, which is constructed with H-profile steel beams; 2) the sprung mass, where lateral steel plates are added to approximate the mass of the quarter chassis; the sprung mass can only translate vertically along a railway, which is attached on the supporting frame; 3) a double wishbone suspension assembly, which is from the actual rear axle of a Ferrari F430 sports car; 4) a road wheel, with its hub carrier connected with the two wishbones, also from the F430; 5) an Öhlins spring-damper unit (TTX40); 6) a single-link variant assembly, which is driven by a rotary actuator; and 7) a cam-driven excitation mechanism with a road plate, which emulates vertical road disturbance.

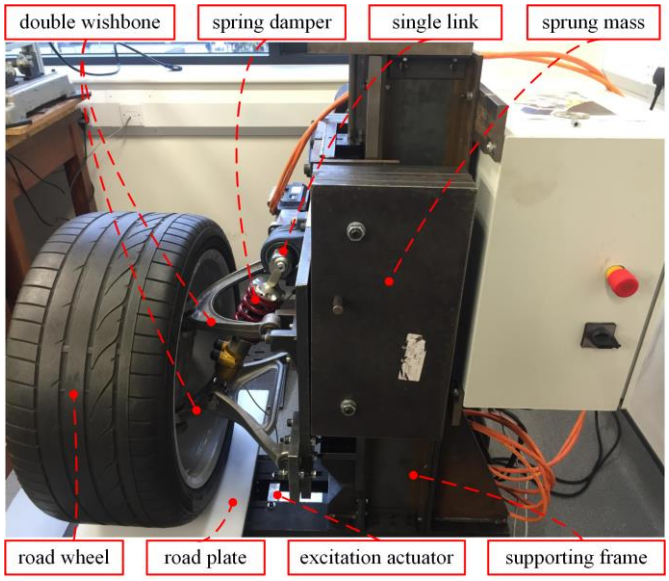

Fig. 2. The SAVGS quarter car test rig.

With regards to the electrical parts, a real-time micro-controller (NI cRIO-9022) is playing the core role for the test rig embedded control and monitoring. This physical controller coordinates other electrical components, including: 1) one servo drive for the single-link actuator, which includes a permanent-magnet synchronous motor (PMSM, Kollmorgen AKM33H, intentionally limited to 500W peak power) with a 40:1 planetary gear stage; 2) another servo drive for the excitation actuator, which is also a PMSM (Kollmorgen AKM54N) equipped with a 20:1 gear stage; 3) a single-axis accelerometer (for the measurement of the sprung mass vertical acceleration); 4) a linear potentiometer (for the measurement of the suspension deflection); and 5) an industrial computer for human-machine interaction.

The benefits of this SAVGS quarter car test rig are: 1) all the mass properties are the same as an actual GT (Ferrari F430); 2) the geometric nonlinearity as well as the installation ratio are considered, as the real double wishbone suspension assembly is utilized and constructed; 3) the road profile can be accurately generated, by means of the cam's position and velocity control; and 4) the system enables real-time control and monitoring.

2.2 Single-Link Variant

The design of the single-link variant is inspired by the "engine crankshaft". As shown in Fig. 3, a transmission shaft is introduced to connect the actuator shaft and the spring-damper upper end eye. This shaft has a "crankpin", which has an offset of l_{SL} = 11 mm (Arana et al., 2015) with respect to the actuator rotary axis. In this way, this "crankpin" acts as the point 'F' (shown in Fig. 1), and it is aligned with the upper end eye of the spring-damper unit. The particular single-link implementation has advantages of structural simplicity, higher stiffness, and compactness.

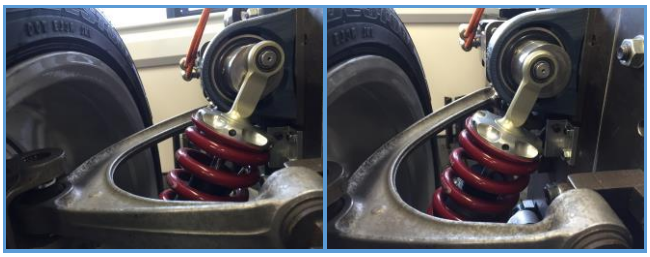

Fig. 3. The single-link variant at the static equilibrium state ($\Delta\theta_{SL} = 0^{\circ}$, left) and the nominal equilibrium state ($\Delta\theta_{SL} = 90^{\circ}$, right).

3. NONLINEAR MODEL IDENTIFICATION

In this section, a theoretical nonlinear quarter car model for the test rig is introduced, with both kinematics and dynamics specified. Combined with the frequency response results obtained through experiments, the model is identified.

3.1 Theoretical Modeling of Quarter Car

Mathematical modeling of the SAVGS quarter car has previously been developed and presented in (Arana, 2015) and (Arana et al., 2015), with the following main features:

1) The kinematics of the multi-body suspension arms, the single-link variant, the road wheel and the quarter car body are described using the multi-body modeling software, *AutoSim* (Anon, 1998).

2) The damping nonlinearity in the spring-damper unit is represented by a look-up table provided by the supplier.

3) A PMSM actuator is selected to drive the single-link. The classical "*d-q*" vector transformation (Hughes et al., 2013) is adopted to mathematically build the actuator models, while a cascaded velocity-torque control algorithm is applied to the single-link motion tracking.

This previous modeling work (referred to as "SimQC" model here) is adopted in the present paper to represent the test rig, which also includes the features of sprung mass-railway friction and wheel tire-road plate friction (model referred to as "SimTR" here), as shown in Fig. 4. These new features need to be identified or approximated through experiments.

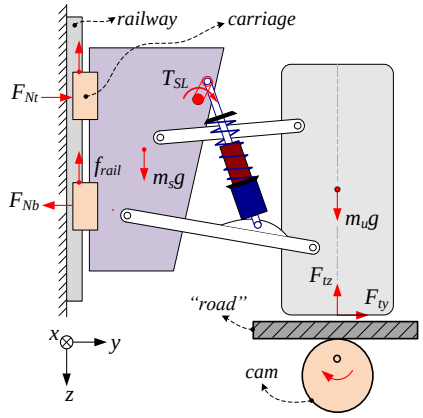

Fig. 4. Schematic of the nonlinear model of the SAVGS quarter car test rig.

3.2 Model Identification for Test Rig

A group of harmonic tests are performed to identify the test rig characteristic in the frequency domain. As shown in Fig. 5, the resonant frequency of the test rig ("Test") is 2.35 Hz, instead of 2 Hz in the theoretical quarter car ("SimQC"); the test rig dynamics are attenuated at around 2 Hz.

In order to compensate the dynamics behavior differences between simulation and experimental results, the "SimQC" quarter car model is extended by the addition of railway and tire friction, as follows:

1) The railway friction is described as:

$$f_{rail} = \mu_r (|F_{Nt}| + |F_{Nb}|), \tag{1}$$

where F_{Nt} is the lateral load acting on the top carriage from the railway, F_{Nb} is the lateral load acting on the bottom carriage from the railway, and μ_r (=0.03) is the friction coefficient between the railway and carriages. The lateral loads on the two carriages can be calculated from the reaction moment in the *x* direction, acting on the sprung mass from the railway (denoted as M_{Nx}) and the lateral reaction force, acting on the sprung mass from the railway (denoted as F_{Ny}). Both M_{Nx} and F_{Ny} can be provided by *AutoSim* functions. The lateral loads on the two carriages are then derived as:

$$F_{Nt} = \frac{M_{Nx}}{l_{tb}} + \frac{F_{Ny}}{2}, F_{Nb} = \frac{M_{Nx}}{l_{tb}} - \frac{F_{Ny}}{2}, \tag{2}$$

where l_{tb} is the vertical distance between the top and the bottom carriages' center.

2) The lateral tire force is relatively complex, as it is related to the vertical tire load, the wheel camber angle, the sideslip, the tire's lateral stiffness, and so on (Jazar, 2013). The lateral force is approximated and simplified using:

$$F_{ty} = \min(1, \frac{|\dot{y}_H|}{\dot{y}_{Hth}}) \times \mu_t |F_{tz}|, \tag{3}$$

where $\dot{y}_H$ is the lateral velocity of the tire contact point with the road plate (point 'H' in Fig. 1), $\dot{y}_{Hth}$ (=0.05 m/s) is a shaping constant, and μ_t (=0.25) is the friction coefficient between the tire and the road plate.

The simulation results of the extended model ("SimTR") are shown in Fig. 5, and it can be seen that they are much closer to the to the test results ("Test") in the frequency domain.

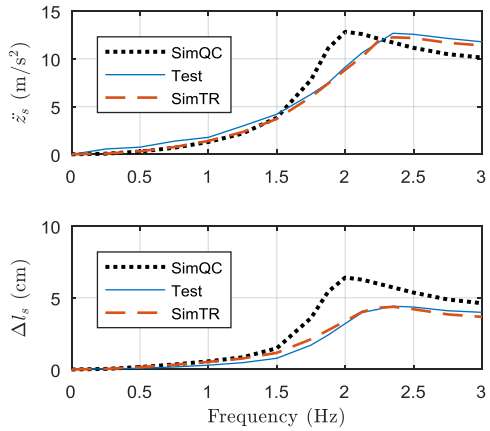

Fig. 5. Frequency response comparison between the theoretical quarter car simulation ("SimQC"), the test results ("Test") and the nonlinear test rig simulation ("SimTR"). The disturbance input is a sinusoidal road displacement with a 2.75 cm peak-to-peak amplitude (constrained by the cam profile). The corresponding sprung mass acceleration (top) and suspension deflection (bottom) are plotted with their peak-to-peak value.

4. CONTROL DESIGN

In this section, a linear equivalent model of the SAVGS quarter car is utilized to synthesize an H-infinity control scheme for the SAVGS operation in the test rig that aims to enhance both the ride comfort and the road holding.

4.1 Linear Equivalent Model

The linear equivalent modeling method for the SAVGS quarter car presented in (Arana, 2015) and (Arana et al., 2017) is adopted in this paper. In this approach the geometric nonlinearity of the SAVGS is compensated and therefore the model is accurate for a large range of single-link angle variations. As shown in Fig. 6, the linear equivalent model is obtained from the nonlinear multi-body model, with α being the conversion function and that also compensates the geometric nonlinearity.

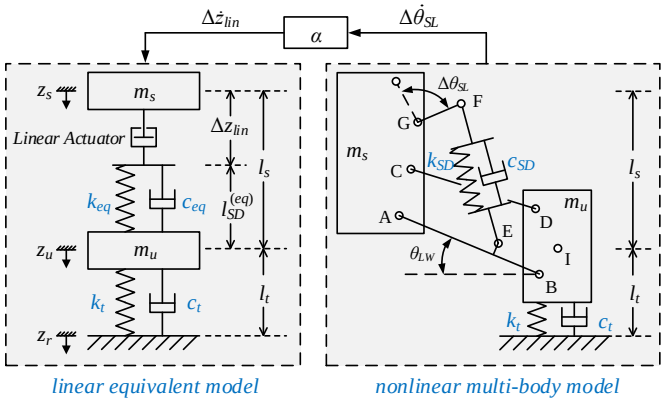

Fig. 6. Linear equivalent model and nonlinear multi-body model. The velocity of the single-link actuator and of the linear equivalent actuator can be converted through block α.

Function α is defined as below:

$$\alpha = \frac{\Delta \dot{z}_{lin}}{\Delta \dot{\theta}_{SL}}, \tag{4}$$

where Δz_{lin} is the displacement increment of the linear actuator, and $\Delta\theta_{SL}$ is the single-link angle increment with respect to its static equilibrium state (shown in Fig. 6).

The linear equivalent model is derived based on the nonlinear multi-body model, with the following assumptions made:

1) Both models have the same suspension deflection ($l_s = z_u - z_s$, defined as the vertical distance between the sprung mass center and the unsprung mass center) and the same tire deflection ($l_t = z_r - z_u$, defined as the vertical distance between the road surface and the unsprung mass center):

$$l_s = \Delta z_{lin} + l_{SD}^{(eq)}, \tag{5}$$

where $l_{SD}^{(eq)}$ is the length of the equivalent spring damper.

2) The single-link rotary actuator and the equivalent linear actuator have the same power output:

$$T_{SL}\dot{\theta}_{SL} = F_{SD}^{(eq)}\Delta \dot{z}_{lin}, \tag{6}$$

where $F_{SD}^{(eq)}$ denotes the equivalent spring force.

3) The equivalent spring satisfies Hooke's law, while the equivalent damper has the same energy dissipation as the real one:

$$\begin{aligned} k_{eq} &= \frac{dF_{SD}^{(eq)}}{dl_{SD}^{(eq)}} \\ c_{eq}\left(\frac{dl_{SD}^{(eq)}}{dt}\right)^2 &= c_{SD}\left(\frac{dl_{SD}}{dt}\right)^2. \end{aligned} \tag{7}$$

The equivalent spring stiffness k_{eq}, the equivalent damping c_{eq} and block α are all functions related to the single-link angle ($\Delta\theta_{SL}$) and the lower wishbone angle (θ_{LW}). They can be derived through equations (5)-(7). k_{eq} and c_{eq} are approximated to constants of 59987 N/m and 2087.4 N/(m/s) respectively. The conversion function α is slightly dependent on θ_{LW}, and it can be approximated to a parabolic equation with respect to $\Delta\theta_{SL}$ only, as shown in Fig. 7.

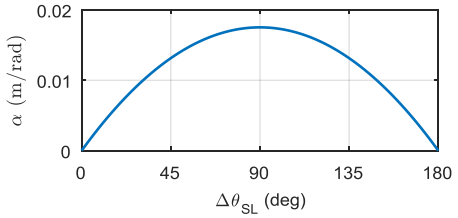

Fig. 7. Approximated model conversion function α against the single-link angle ($\Delta\theta_{SL}$).

The linear equivalent model of the SAVGS is finally given:

$$\begin{aligned} m_s\ddot{z}_s &= k_{eq}(\Delta l_s - \Delta z_{lin}) + c_{eq}(\Delta \dot{l}_s - \Delta \dot{z}_{lin}) \\ m_u\ddot{z}_u &= -k_{eq}(\Delta l_s - \Delta z_{lin}) - c_{eq}(\Delta \dot{l}_s - \Delta \dot{z}_{lin}) + k_t\Delta l_t + c_t\Delta \dot{l}_t. \end{aligned} \tag{8}$$

4.2 H-infinity Control

H-infinity control is widely adopted for active suspensions, as it is robust for applications to multi-input multi-output (MIMO) systems. The standard configuration for the H-infinity controller synthesis is illustrated in Fig. 8.

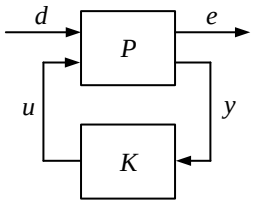

Fig. 8. Generalized regulator configuration of the H-infinity control application. P is a linear plant in state-space representation, K is the synthesized H-infinity controller, d corresponds to the exogenous disturbances, u to the manipulated variables, e to the performance objectives to be minimized, and y to the system measurements for feedback (Zhou et al., 1998).

The H-infinity control synthesis scheme for the SAVGS quarter car, shown in Fig. 9, is based on the work in (Arana, 2015) and (Arana et al., 2016), with the following modifications made to adapt it to the test rig:

1) Two of the disturbance inputs are used, $d = [d_1\ d_2]$. d_1 is an external reference signal of the linear equivalent actuator displacement, $\Delta z_{lin(e)}$, to enable zero or low frequency tracking, for example to set the nominal position of the single-link, and d_2 is the vertical road velocity. The load transfer disturbance is not included here, as it cannot be implemented by the rig.

2) Given the availability of the sensors in the test rig, the system measurements are selected as: $y = [y_1\ y_2\ y_3]$, which are the suspension deflection, the sprung mass acceleration, and the displacement of the equivalent linear actuator (converted from the measurement of the single-link rotary encoder).

3) The objective weighting functions W_{Acc} and W_{TD} are tuned to make the controller take effect below human-sensitive frequency (5 Hz) and wheel resonant frequency (10 Hz) respectively, while W_{eff} penalizes the control effort above 10 Hz, where also the accelerometer noise concentrates.

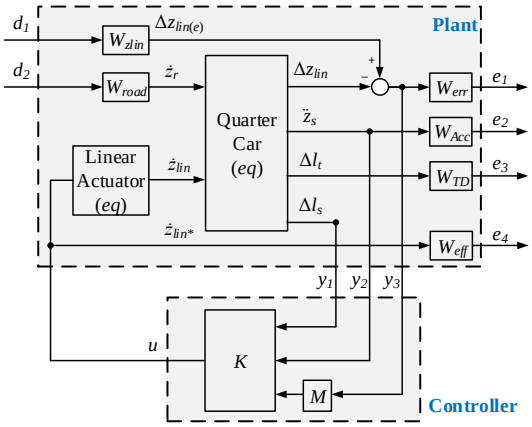

Fig. 9. The H-infinity controller synthesis in the SAVGS quarter car. "Quarter Car (*eq*)" is the linear equivalent model of the SAVGS quarter car, which is the state-space representation of equation (8). "Linear Actuator (*eq*)" is a first-order transfer function with the cut-off frequency of 17.8 Hz (Arana et al., 2017). Variables [*d*], [*e*], [*y*] and [*u*] correspond to those in Fig. 8. '*K*' is the generated H-infinity controller. Block '*M*' is utilized to zero the single-link angle tracking error 'e_1'. [W_{zlin} W_{road}] are disturbance weighting functions for the external reference of the linear equivalent actuator displacement ($\Delta z_{lin(e)}$) and the road disturbance respectively. [W_{err} W_{Acc} W_{TD} W_{eff}] are objective weighting functions for the single-link angle tracking error, the sprung mass acceleration, the tire vertical deflection and the control effort respectively.

The weighing functions of the disturbance inputs are:

$$W_{road} = 0.25, W_{zlin} = 0.02 \cdot \frac{1}{\frac{s}{2\pi \cdot 1} + 1}. \tag{9}$$

The weighing functions of the objectives are tuned as:

$$W_{err} = \frac{1}{0.004} \cdot \frac{\frac{s}{2\pi \cdot 120} + 1}{\frac{s}{2\pi \cdot 0.3} + 1}, W_{Acc} = \frac{1}{3} \cdot \frac{1}{\frac{s}{2\pi \cdot 10} + 1}$$
$$W_{TD} = \frac{1}{0.005} \cdot \frac{1}{\frac{s}{2\pi \cdot 5} + 1}, W_{eff} = \frac{1}{0.1} \cdot \frac{(\frac{s}{2\pi \cdot 10} + 1)^2}{(\frac{s}{2\pi \cdot 1000} + 1)^2}. \tag{10}$$

The block '*M*' (Zhou et al., 1998) has been chosen as:

$$M = \frac{\frac{s}{2\pi \cdot 1} + 1}{s}. \tag{11}$$

The H-infinity controller '*K*', together with block '*M*', are finally used to provide the velocity reference for the single-link actuator in the SAVGS quarter car test rig.

5. EXPERIMENTS

This section discusses the SAVGS experimental testing. Results related to ride comfort and suspension deflection are presented, and are also used to further validate the accuracy of the quarter car model.

5.1 Tests over Harmonic Road

The road profile is generated by the cam-driven excitation mechanism in the test rig. Due to the inherent space constraint, the cam utilized implements a road height variation with 2.75 cm peak-to-peak amplitude.

The other disturbance input, shown as $\Delta z_{lin(e)}$ in Fig. 9, is fixed at the value of its nominal state $\Delta z_{lin}^{(ne)}$ (corresponds to $\Delta\theta_{SL} = 90^{\circ}$), where the single-link has maximum influence on the suspension dynamics (Arana, 2015).

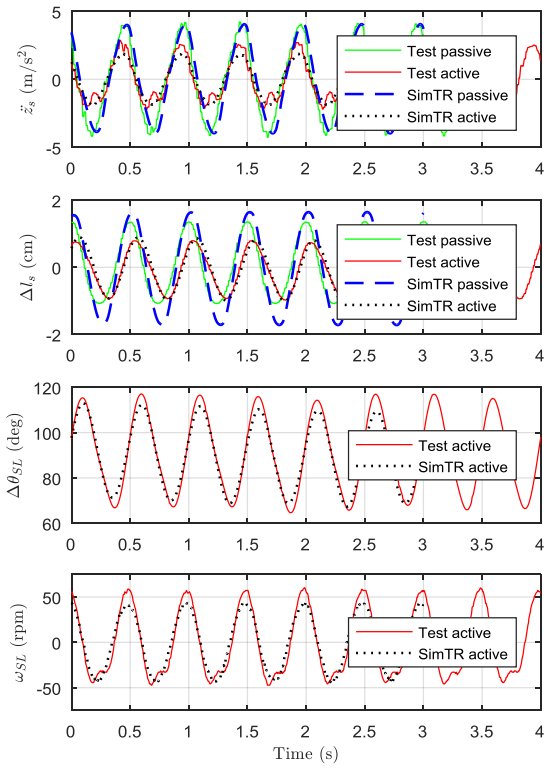

Fig. 10. Test results over a harmonic road profile, with 2 Hz frequency and 2.75 cm peak-to-peak amplitude. The variables depicted are (top to bottom): sprung mass vertical acceleration, suspension deflection, single-link angle, and single-link velocity.

Tests with a 2 Hz harmonic road profile are first conducted, as this frequency is thought to be human sensitive. As shown in Fig. 10, the comparison between "Test passive" and "Test active" demonstrates that the actively controlled single-link significantly contributes to the suspension performance. The RMS value of the sprung mass vertical acceleration and the suspension deflection are reduced by 41.44% and 31.11% respectively. On the other hand, the results of "Test" and "SimTR" are well matched, despite the largest discrepancy occurring in the suspension deflection, thus the identified and approximated nonlinear model is considered to be accurate.

5.2 Tests over Frequency Sweep Excitation

A road profile with swept frequency is tested to present the SAVGS response in the frequency domain. The peak-to-peak

value of the road height variation is 2.75 cm, while the road excitation frequency increases linearly from 0 Hz to 3 Hz in a time period of 60 s.

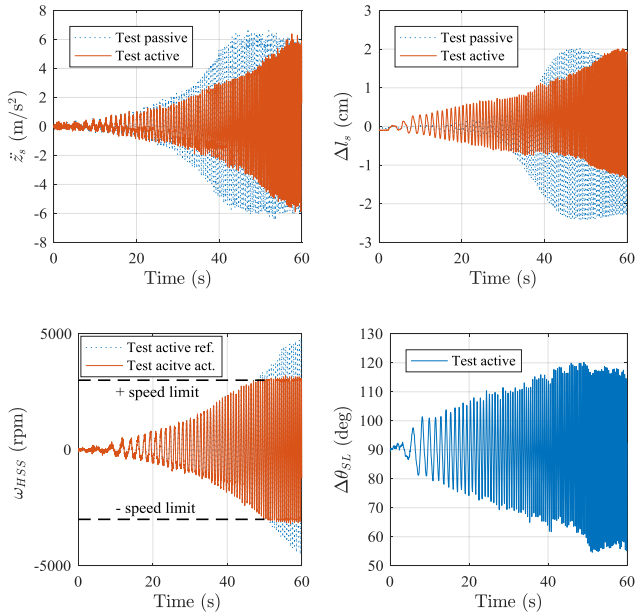

Fig. 11. Frequency sweep test results. Variables depicted are sprung mass vertical acceleration, suspension deflection, single-link actuator velocity (of the gearbox high-speed shaft), and single-link angle.

Both the sprung mass acceleration and the suspension deflection (top-left and top-right in Fig. 11) are significantly attenuated by the SAVGS at the human-sensitive frequency range around 2-3 Hz (40-60 s). The motion of the single-link (bottom-right in Fig. 11) demonstrates that the actuator as well as its controller accurately track the reference velocity (0-50 s). While the road disturbance is above 2.5 Hz (50-60 s), the actual speed of the actuator is saturated at 3000 rpm, because of the speed limit in the velocity loop, which is in place to protect the actuator. The corresponding single-link angle ranges between 55˚ and 120˚ (bottom-right in Fig. 11).

6. CONCLUSIONS

A single-link variant of the Series Active Variable Geometry Suspension is designed and implemented in a test rig. Starting from a theoretical quarter car model, the friction nonlinearities that exist in the rig are identified through the test results in the frequency domain and added to the model. Further utilizing a linear equivalent model, an H-infinity controller is synthesized and adapted to the rig application.

The experimental study over the quarter car test rig indicates the initial feasibility of the SAVGS: the vehicle dynamics, including the sprung mass vertical acceleration and the suspension deflection, are significantly attenuated at around 2 Hz; the H-infinity controller is proven to be robust, despite the effect of friction, sensor noise, and other factors.

In future work, SAVGS quarter car experiments will be performed over different road profiles (e.g. speed bump and ISO random road). Full car control algorithms for the operation of the single-links at four corners of the car will also be developed for the chassis attitude adjustment. Full car tests on the road will then be conducted.

REFERENCES

Anon. (1998). *AutoSim 2.5+ Reference Manual*, Mechanical Simulation Corporation, Ann Arbor MI, USA. [Online]. Available: http://www.carsim.com.

Arana, C., Evangelou, S. A. & Dini, D. (2015) Series active variable geometry suspension for road vehicles. *IEEE/ASME Transactions on Mechatronics.* 20 (1), 361-372.

Arana, C., Evangelou, S. A. & Dini, D. (2017) Series active variable geometry suspension application to comfort enhancement. *Control Engineering Practice.* 59, 111-126.

Arana, C., Evangelou, S. A. & Dini, D. (2014) Car attitude control by series mechatronic suspension. *IFAC Proceedings Volumes.* 47 (3), 10688-10693.

Arana, C. (2015). *Active variable geometry suspension for cars*. Ph.D. dissertation, Dept. Elect. Eng. and Mech. Eng., Imperial College London.

Dixon, J. C. (2009) *Suspension geometry and computation.* , John Wiley & Sons.

Elbeheiry, E. M., Karnopp, D. C., ElAraby, M. E. & Abdelraaouf, A. M. (1995) Advanced ground vehicle suspension systems-a classified bibliography. *Vehicle System Dynamics.* 24 (3), 231-258.

Evangelou, S., Kneip, C., Dini, D., De Meerschman, O., Palas, C. & Tocatlian, A. (2011) *Variable-Geometry Suspension Apparatus and Vehicle Comprising such Apparatus*. US9026309B2.

Fischer, D. & Isermann, R. (2004) Mechatronic semi-active and active vehicle suspensions. *Control Engineering Practice.* 12 (11), 1353-1367.

Hughes, A. & Drury, B. (2013) *Electric motors and drives: fundamentals, types and applications.* , Newnes.

Jazar, R. N. (2013) *Vehicle dynamics: theory and application.* , Springer Science & Business Media.

Sharp, R. & Crolla, D. (1987) Road vehicle suspension system design-a review. *Vehicle System Dynamics.* 16 (3), 167-192.

Zhou, K. & Doyle, J. C. (1998) *Essentials of robust control.* , Prentice hall Upper Saddle River, NJ.

APPENDIX

Table I. Main Parameters of Quarter Car Test Rig

Parameters	Symbol	Value	Unit
Weight of sprung mass	m_s	320	kg
Weight of unsprung mass	m_u	49	kg
Spring stiffness	k_{sd}	157614	N/m
Linearized damping	c_{sd}	5792	N/(m/s)
Tire's radial stiffness	k_t	2.75e5	N/m
Tire's radial damping	c_t	300	N/(m/s)
Single-link actuator gear ratio	R_{GB}	40	-
Single-link length	l_{SL}	11	mm